Journal of Machine Engineering, 2026, Vol. 26
ISSN 1895-7595 (Print) ISSN 2391-8071 (Online)

Received*: 17 May 2026* /Accepted: *22 June 2026* / Published online: *26 September 2026*

process monitoring,
structural response,
compliance matrix
AWJ

Tomasz WALA[1*]

LOAD IDENTIFICATION IN ABRASIVE WATERJET CUTTING USING A FEM-DERIVED COMPLIANCE MATRIX AND STRUCTURAL RESPONSE ANALYSIS

This paper presents a methodology for describing the relationship between forces acting on the cutting head of an abrasive waterjet machine and the structural response of its supporting structure. The study was conducted in two stages. First, experimental measurements of reaction forces during high-pressure AWJ cutting were performed to determine the influence of process parameters and define the loading conditions. Next, a finite element (FEM) model of the supporting structure was developed, in which the cutting head was idealized as a reference point to enable controlled loading in three directions. A series of simulations with unit loads was carried out to determine the compliance matrix of the structure. The model allows rapid prediction of sensor displacements for arbitrary force combinations without repeated FEM analyses. Experimental validation showed good agreement, with a relative error of approximately 8% in the direction of the lowest stiffness, demonstrating the applicability of the proposed approach for monitoring loads in AWJ processes.

1. LITERATURE REVIEW

The abrasive waterjet (AWJ) cutting process has been extensively studied due to the complexity of the physical phenomena occurring in the interaction zone between the jet and the workpiece material. Review papers indicate that process performance and cutting stability strongly depend on technological parameters, in particular traverse speed, jet pressure, and abrasive mass flow rate [1].

The influence of process parameters on the geometric and surface quality characteristics of the cut has been widely investigated in studies such as [2, 3]. These works demonstrate that variations in traverse speed affect not only kerf width and surface roughness, but also the nature of dynamic interactions between the jet and the material. This indirectly indicates that the reaction forces acting on the cutting head vary during the AWJ process.

Direct investigations of jet–material interactions, including the characterization of impact forces, have been reported in [4, 5]. The results confirm that the magnitude and distribution of forces generated during cutting are complex and depend on multiple process parameters, while their direct measurement under industrial conditions remains challenging.

---

[1] Department of Machine Technology, Silesian University of Technology in Gliwice Faculty of Mechanical Engineering, Poland
[*] E-mail: tomasz.wala@polsl.pl
https://doi.org/10.36897/jme/224894

For this reason, increasing attention has been devoted to indirect monitoring methods based on the analysis of dynamic responses of the process or machine structure. Examples include studies [6, 7], where the state of the cutting process was evaluated using acoustic emission and vibration signals. Similar approaches were presented in [8, 9], where acoustic emission (AE) signals were used to predict cutting depth and process stability.

A significant group of studies also focuses on vibrations of the cutting head and their influence on cutting performance. In works [10, 11], it was demonstrated that vibration characteristics of the cutting head are directly correlated with kerf geometry and surface features. These findings suggest that the dynamic response of the supporting structure can serve as a valuable source of information about the AWJ process.

The issue of monitoring the condition of head components, particularly the focusing tube, has been investigated in studies such as [12, 13]. The authors showed that measurements of vibrations or structural deformations can provide an effective diagnostic tool, offering an alternative to direct force measurements. In the context of sensor selection, studies comparing piezoelectric and strain-based sensors indicate that piezoelectric sensors, due to their high sensitivity and the possibility of direct mounting on machine structures, are particularly suitable for monitoring the dynamic response of mechanical systems [14].

At the same time, advanced numerical methods for modeling the AWJ process have been developed, including CFD, FEM, and DEM approaches [15, 16]. Although these models enable detailed analysis of erosion mechanisms and particle interactions, their high computational cost limits their direct application in industrial monitoring systems.

Despite the extensive research on AWJ processes, monitoring techniques, and numerical modeling, there is still a lack of approaches that combine experimentally determined force ranges with a simplified and physically interpretable model of the structural response of the cutting head support. In particular, no methods have been reported in which the relationship between forces Fx, Fy, and Fz and the response measured at the location of a sensor mounted on the cutting head is expressed in the form of a compact matrix model.

Existing studies primarily focus either on direct force measurements or on process monitoring techniques. Relatively little attention has been devoted to utilizing structural-response signals already available in industrial AWJ systems for indirect load identification and model-based interpretation of cutting-head support behaviour.

The approach presented in this work, based on finite element analysis of the supporting structure and the determination of a compliance matrix relating the acting forces to the displacement response of a piezoelectric sensor, addresses this gap and contributes to the advancement of current knowledge. The novelty of this work lies in the formulation of a compact compliance-matrix-based model enabling the prediction of structural response at the sensor location based on experimentally determined force components, combining experimental force characterization with FEM-based modeling.

2. RESEARCH METHODOLOGY

The study presented in this paper was divided into two main stages. In the first stage, experimental measurements of reaction forces generated during abrasive waterjet cutting were performed using a Kistler dynamometer. The objective of this stage was to determine representative values of the force components acting during the cutting process and to evaluate the influence of selected technological parameters, particularly the traverse speed, on their magnitude. The forces were considered in a Cartesian coordinate system along the *X*, *Y*, and *Z* directions.

The experimentally determined force components were subsequently used as input data for the second stage of the study, which focused on numerical modelling of the cutting-head supporting structure. Due to the complex geometry of the system and the limited accessibility for direct deformation measurements in the actual structure, a finite element method (FEM) approach was adopted.

The objective of the numerical study was to develop an FEM model of the supporting structure capable of predicting the structural response at the location of the factory-installed M240 PCB sensor as a function of forces acting along the *X*, *Y*, and *Z* axes. A linear relationship between the applied loads and the resulting displacements at the sensor location was assumed. Based on a series of FEM simulations, a compliance matrix describing the relationship between the applied forces and the resulting structural response was determined.

The relative displacements predicted by the FEM model were subsequently converted into equivalent strain values according to the geometrical characteristics of the M240 PCB sensor. In the final stage, the strain values predicted by the FEM-based compliance model were compared with the sensor signals recorded during actual abrasive waterjet cutting experiments. This comparison served as a validation of the proposed modelling approach and allowed assessment of the applicability of the compliance-matrix-based framework for describing the structural response of the cutting-head support.

3. EXPERIMENTAL FORCE MEASUREMENTS IN AWJ CUTTING

As part of the preliminary study, an experimental setup was developed to measure reaction forces generated during high-pressure abrasive waterjet cutting for two representative workpiece materials.

The objective of this stage was to determine the influence of a selected technological parameter, namely the traverse speed of the cutting head, on the force components generated during the cutting process.

The forces were measured using a Kistler 9272 dynamometer (Fig. 1), on which the workpiece was mounted. The process parameters kept constant during the experiments were the jet pressure of 330 MPa and the abrasive mass flow rate of 340 g/min. The tests were conducted for two materials: aluminium alloy EN-AW-7075 and carbon steel S235RJ. The thickness of the specimens was 20 mm. The experiments were performed on a Waterjet HWM-P1520/1-3D machine.

The cutting head was equipped with a sapphire water orifice of 0.35 mm diameter and a focusing tube of 1.0 mm diameter. During all tests, a constant stand-off distance of 2 mm between the focusing tube outlet and the workpiece surface was maintained. Australian Garnet abrasive with a mesh size of #80 was used throughout the experiments.

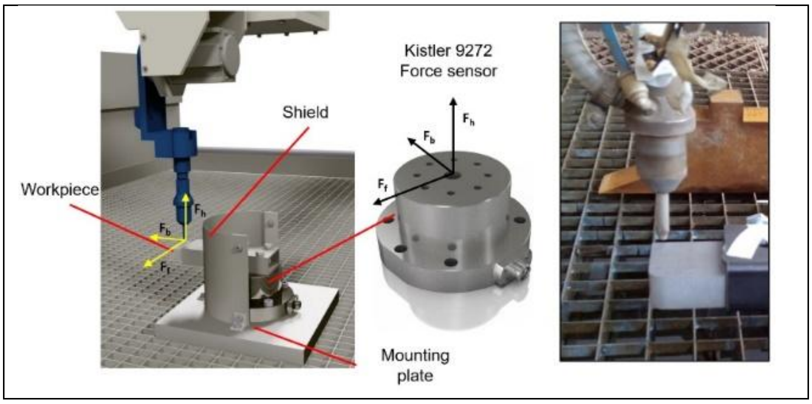

Fig. 1. Experimental setup for force measurements during high-pressure abrasive waterjet cutting

The cutting process was performed along the *Y*-axis, corresponding to the feed force component F_f. The experimental results (Table 1 and Table 2) showed that the traverse speed has the most significant influence on the force component in the *Y* direction (F_f) and on the component F_h, which is normal to the upper surface of the workpiece (*Z* direction). The component F_b corresponds to the lateral interactions acting in the direction normal to the cutting surface (*X* direction). The force components F_f, F_h, and F_b correspond to the global force components F_y, F_z, and F_x, respectively.

Table 1. Values of average reaction forces when cutting 20 mm thick aluminium EN-AW-7075

Feed rate [mm/min]	Force F_b [N]	Force F_f [N]	Force F_h [N]
98	0.03	3.99	2.35
137	0.57	3.93	2.34
217	0.46	9.06	3.31
304	0.12	10.57	9.46

Table 2. Values of average reaction forces during cutting of 20 mm thick carbon steel S235RJ

Feed rate [mm/min]	Force F_b [N]	Force F_f [N]	Force F_h [N]
24	0.13	3.88	1.3
31	0.08	5.46	1.74
43	0.22	7.38	3.65
68	0.01	8.2	4.74

The experimentally determined force components were subsequently used as input loads for the FEM model of the cutting-head supporting structure. In this way, the measured force ranges provided the basis for establishing realistic loading conditions in the numerical analyses and for determining the compliance matrix of the investigated system.

4. FEM MODEL OF THE SUPPORTING STRUCTURE

The object of the study is the mounting system of the cutting head of a Waterjet HWM-P1520/1-3D machine used in the experimental investigations. The analyzed structure is responsible for transferring static and dynamic loads generated during the abrasive waterjet cutting process. The investigated Waterjet HWM-P1520/1-3D machine is equipped with a five-axis CNC control system enabling both conventional 2D cutting and spatial machining operations. The cutting head assembly incorporates additional rotational B and C axes, allowing the orientation of the cutting jet to be adjusted with respect to the workpiece. Such functionality enables bevel cutting, taper compensation, and the execution of complex three-dimensional cutting trajectories. Compared to conventional three-axis AWJ systems, the introduction of additional rotational axes requires a more complex supporting structure of the cutting head. Consequently, the stiffness and compliance characteristics of the supporting assembly become important factors affecting the positioning accuracy of the cutting jet and the overall cutting process. For this reason, the cutting-head support structure was selected as the object of the present investigation.

The numerical model is based on the actual industrial configuration of the machine. An M240 PCB sensor is factory-installed on the supporting structure of the cutting head as part of the machine monitoring and collision-detection system (Fig. 2).

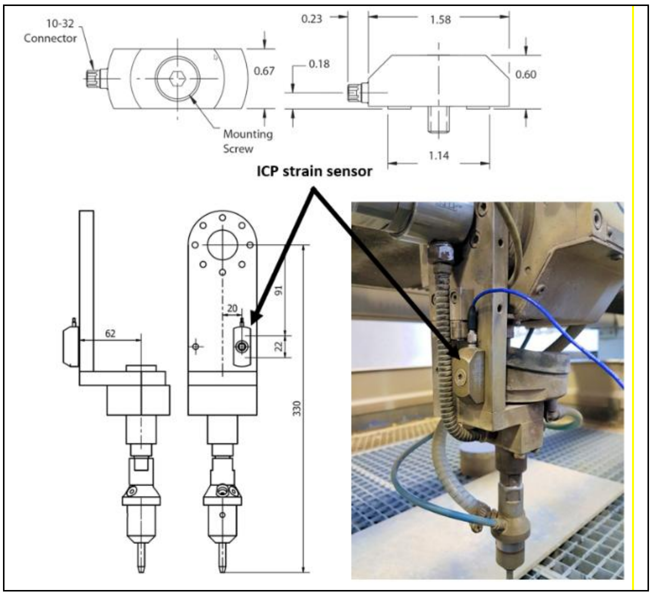

Fig. 2. Mounting of the cutter-head collision detection sensor in the supporting structure of the AWJ machine

The numerical model represents a selected part of the structure corresponding to the supporting system of the cutting head. The cutting head itself was replaced by an idealized element. The simplification of the cutting head geometry by a reference point allows for a controlled and unambiguous application of loads, while avoiding additional geometric and contact nonlinearities that are not essential for the considered problem.

The tip of the cutting head was modeled as a reference point (RP), denoted as POINT_FORCE, to which external forces were applied in three orthogonal directions. The following correspondence between the experimental and global force components was assumed: $F_x \leftrightarrow F_b$, $F_y \leftrightarrow F_f$, $F_z \leftrightarrow F_h$ (Fig. 3). The force components F_b, F_f and F_h were obtained experimentally using the Kistler dynamometer and subsequently used as loading conditions in the FEM model.

The connection between the POINT_FORCE reference point and the supporting structure was defined using coupling constraints, which can be interpreted as ideal elements transferring loads to selected structural surfaces. The reference point was coupled with surfaces representing the actual load transfer regions within the mounting assembly.

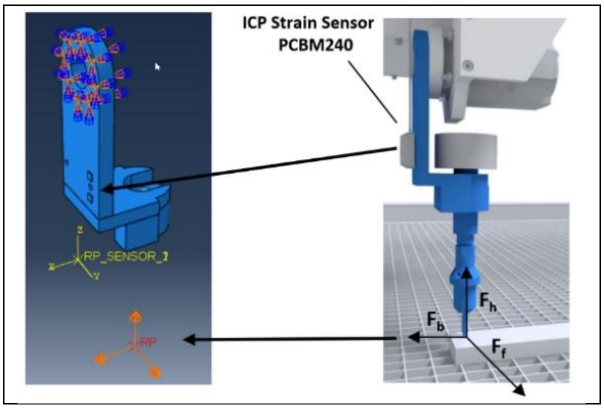

Fig. 3. FEM model of the supporting structure corresponding to the actual five-axis cutting head support assembly

This modeling approach enables:

- transfer of forces from the idealized representation of the cutting head to the structural surfaces,
- a clear definition of loading directions,
- reduction of local stress concentrations associated with detailed geometric modeling of the cutting head.

The analysis was performed under the assumption of small deformations and linear elastic material behavior. The numerical simulations were performed using the Abaqus software package (Dassault Systèmes), employing a linear static analysis procedure with the Abaqus/Standard solver. The modelling workflow included geometry preparation, boundary condition definition, coupling constraints, and postprocessing of displacement responses.

4.1. BOUNDARY CONDITIONS AND MATERIAL PROPERTIES

The numerical model includes structural components responsible for load transfer within the cutting head mounting system. The surfaces corresponding to the connection with the machine frame were constrained by removing all degrees of freedom, representing a fully fixed support condition in the actual structure. Contact between selected surfaces was modeled using tie constraints, ensuring no relative motion between the connected parts. This assumption is justified by the nature of the connections within the considered load range, where separation or sliding does not occur. The structural material was assumed to be homogeneous, isotropic, and linearly elastic, representing stainless steel with Young's modulus $E = 200$ GPa and Poisson's ratio $\nu = 0.3$. A mesh convergence study was performed to ensure that the displacement results at the sensor location were not significantly affected by further mesh refinement. These assumptions are consistent with the linear static analysis framework adopted in this study.

4.2. DEFINITION OF VIRTUAL DISPLACEMENT SENSORS

To enable direct comparison between numerical results and experimental measurements, virtual displacement sensors were introduced in the numerical model. The sensors were defined as reference points kinematically coupled with surfaces denoted as SENSOR_1 and SENSOR_2 (Fig. 4). The quantity of interest was the relative displacement between these two points, defined as:

$$\Delta \mathrm{U}(t) = \mathrm{U}_{S2}(t) - \mathrm{U}_{S1}(t) \tag{1}$$

where $\mathrm{U} = [U_x, U_y, U_z]^T$ represents the displacement vector in the global coordinate system.

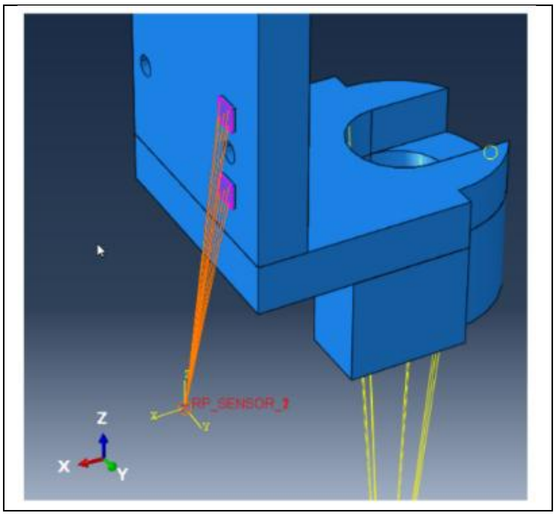

Fig. 4. View of virtual sensors mounted on the supporting structure

At each increment of the analysis, the solver computes the displacement vectors of the reference points associated with the sensor ends:

$$\mathbf{U}_{S1} = [U_{x,S1}(t), U_{y,S1}(t), U_{z,S1}(t)]^T \tag{2}$$

$$\mathbf{U}_{S2} = [U_{x,S2}(t), U_{y,S2}(t), U_{z,S2}(t)]^T \tag{3}$$

The M240 PCB sensor does not directly measure force components acting on the cutting head. Instead, its output is related to the deformation of the supporting structure. Therefore, in the present study, the FEM model was used to determine the relative displacement between the sensor attachment points. The calculated displacement values were subsequently converted into equivalent strain values according to the geometrical characteristics of the sensor and compared with the experimentally recorded sensor response. In this way, the relative displacement between the sensor attachment points constitutes the underlying mechanical quantity predicted by the FEM model, whereas the sensor output is recorded in the form of strain-related quantities. This formulation establishes a direct link between the numerical prediction of structural response and the experimentally measured sensor signal.

4.3. ANALYSIS METHODOLOGY AND GOVERNING EQUATIONS

The analysis was performed under the assumptions of linear static conditions, small displacements, and linear elastic material behaviour. The linear formulation was adopted as a first-order approximation, valid within the considered load range, where no significant nonlinear effects were observed. Under these conditions, the relationship between the forces applied at the POINT_FORCE reference point and the relative displacements measured by the virtual sensor can be expressed as:

$$\Delta\mathrm{U} = \mathrm{A\,F} \tag{4}$$

where $F = [F_x, F_y, F_z]^T$ is the vector of applied forces, and **A** is the compliance matrix of the system.

The relative displacement vector ΔU constitutes the primary mechanical response predicted by the FEM model. For comparison with the experimental measurements obtained from the M240 PCB sensor, the calculated displacements were subsequently transformed into equivalent strain values according to the geometrical characteristics of the sensor. This approach enables a direct comparison between the numerical prediction of the structural response and the experimentally recorded sensor signal. An example of displacement fields of the supporting structure in the *X, Y*, and *Z* directions is presented in Fig. 5.

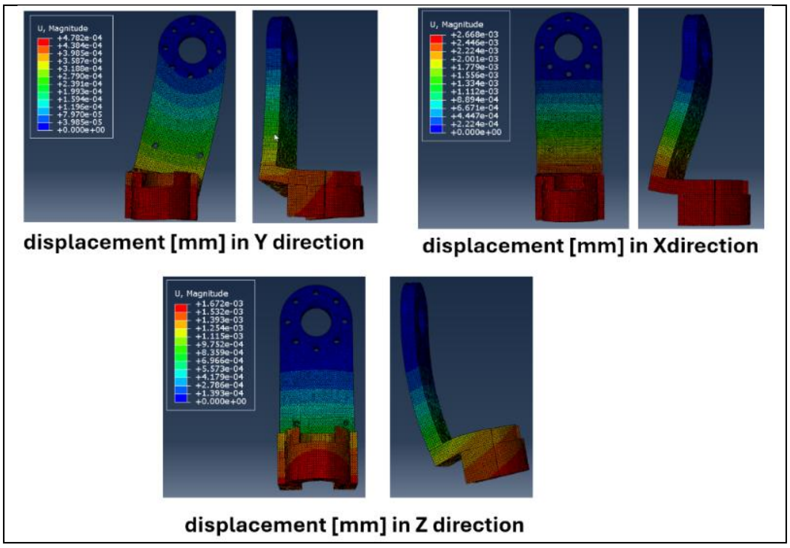

Fig. 5. Example displacement fields of the cutting head supporting structure in X, Y and Z directions

Due to the multi-directional nature of the loading conditions, a single analysis is not sufficient to fully describe the load–response relationship of the supporting structure. Therefore, three independent FEM analyses were performed, in which unit loads were applied successively along the *X*, *Y*, and *Z* directions. The resulting displacement vectors ΔU form the columns of the compliance matrix, which enables prediction of the structural response for arbitrary combinations of forces within the assumed linear range.

This approach allows for a clear identification of the influence of each force component on the displacement response at the sensor location. Moreover, it enables the application of the superposition principle to predict the structural response for arbitrary loading conditions within the assumed linear regime. This formulation provides a compact and computationally efficient representation of the structural response, eliminating the need for repeated numerical analyses.

4.4. COMPLIANCE MATRIX REPRESENTATION AND DISPLACEMENT MODEL

The compliance matrix A is defined as:

$$\mathbf{A} = \begin{bmatrix} A_{11} & A_{12} & A_{13} \\ A_{21} & A_{22} & A_{23} \\ A_{31} & A_{32} & A_{33} \end{bmatrix} \tag{5}$$

where: the coefficient A_{ij} represents the displacement in direction i caused by a unit force applied in direction j.

The units of the matrix coefficients are mm/N. The matrix contains both diagonal terms, corresponding to direct responses, and off-diagonal terms, representing coupling between directions resulting from the geometry and boundary conditions of the structure. To extract the sensor response from the FEM results, a postprocessing procedure based on exporting displacement histories of the reference points associated with SENSOR_1 and SENSOR_2 to CSV format was applied. The relative displacement of the virtual sensor was calculated as:

$$\Delta \mathrm{U}(t) = \mathrm{U}_{S2}(t) - \mathrm{U}_{S1}(t) \tag{6}$$

The algorithm used for determining the compliance matrix based on a series of unit-load analyses and subsequent data processing is illustrated in Fig. 6.

The displacement components ΔU_x, ΔU_y, and ΔU_z were recorded in a tabular form, where each column corresponds to the response to a unit load applied in a given direction. In this way, each column of the table represents one column of the compliance matrix.

Once the compliance matrix A has been determined, the structural response corresponding to any arbitrary force configuration can be calculated using the matrix relation $\Delta U = AF$, without the need for additional FEM analyses.

The compliance matrix obtained from the FEM analyses was exported to a CSV file to enable efficient implementation of the displacement prediction model. The CSV representation serves as a practical realization of the compliance-matrix-based approach and allows rapid evaluation of the structural response without performing additional FEM simulations (Fig. 7).

The use of the CSV format enables a clear and automated transformation of the results of individual FEM analyses into a compact mathematical model describing the structural response. In practice, this means that once the compliance matrix has been determined, further analyses of the influence of loads on sensor displacements can be performed without the need for additional numerical simulations, relying solely on simple matrix operations.

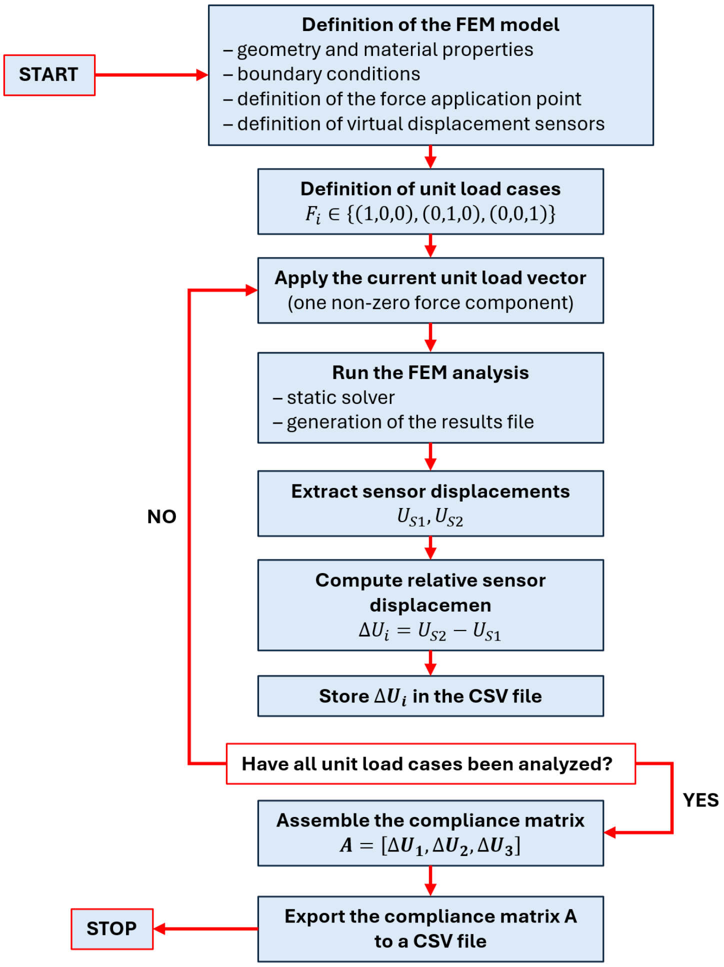

Fig. 6. Block diagram of the algorithm for determining the compliance matrix based on FE analyses and CSV export

Matrix *A* (mm/N): dU = *A* · F
The 3×3 matrix values (the compalaince_matrix.csv).

	Fx	*Fy*	*Fz*
dU1	1.877142E-04	-2.195190E-05	-4.539854E-05
dU2	2.376377E-06	1.002272E-05	-5,521007E-07
dU3	-1.180623E-05	-1.722816E-06	2.974609E-06

• Columns are responses to 1 N in Fx/Fy/Fz.
• dU = A·F for any (*Fx*,*Fy*,*Fz*) in linear range.

Fig. 7. CSV representation of the compliance matrix *A* used for implementation of the displacement prediction model

Consequently, for any combination of force components, the corresponding relative displacements of the virtual sensor can be directly evaluated (Fig. 8).

For consistency with the experimentally recorded M240 PCB sensor output, the relative displacements predicted by the FEM model were converted into equivalent strain values according to the relation:

$$\varepsilon = \frac{dU}{U} \tag{7}$$

where U denotes the characteristic sensor length (see Fig. 2).

Sensor displacement model (linear): dU = A · F
Units: Forces in N. Displacements dU in mm (Abaqus N–mm).

Inputs (change these)

Fx [N]	10	Tip: This linear model is valid only within the linear response range of the FE model.
Fy [N]	10	
Fz [N]	100	
Outputs (computed)		
dU1 (X) [mm]	-2.882231E-03	Definition: dU = U(SENSOR_2) − U(SENSOR_1) Source: last history value in Step-1 for each RP.
dU2 (Y) [mm]	6.878090E-05	
dU3 (Z) [mm]	1.621705E-04	
dL (3D) [mm]	2.887609E-03	

Fig. 8. Example of the sensor displacement model based on the compliance matrix (CSV implementation)

An example of calculated equivalent strain values is presented in Table 3, together with the corresponding FEM-based relationship between equivalent sensor strain and applied force components (Fig. 9). For clarity, the equivalent strain quantities ε_1, ε_2 and ε_3 correspond to the structural responses associated with the force components F_b, F_f and F_h, respectively. These quantities were calculated from the relative displacements predicted by the FEM model according to Eq. (7) and represent the strain-related response that would be observed by the M240 PCB sensor for loading applied predominantly in the *X*, *Y* and Z directions.

Table 3. Calculated equivalent strain values based on the FEM model

factor k	Force $k \cdot F_b$ [N]	Force $k \cdot F_f$ [N]	Force $k \cdot F_h$ [N]	relative disp. ε_1	relative disp. ε_2	relative disp. ε_3
0	0	0	0	0	0	0
0.1	1	1	1	0.05397477	0.005312554	0.00473293
0.2	2	2	2	0.107949541	0.010625108	0.00946586
0.3	3	3	3	0.161924311	0.015937662	0.01419879
0.4	4	4	4	0.215899081	0.021250216	0.01893172
0.5	5	5	5	0.269873852	0.026562771	0.02366465
0.6	6	6	6	0.323848622	0.031875325	0.02839758
0.7	7	7	7	0.377823392	0.037187879	0.033130511
0.8	8	8	8	0.431798162	0.042500433	0.037863441
0.9	9	9	9	0.485772933	0.047812987	0.042596371
1.0	10	10	10	0.539747703	0.053125541	0.047329301

$*\varepsilon = \frac{dU}{U}$. where U is the characteristic length of the sensor (see Fig. 2)

The obtained linear characteristics represent a graphical interpretation of the compliance matrix A. where the slopes of the curves correspond to its coefficients. thus providing a direct link between the applied forces and the predicted structural response of the cutting-head support. The proposed formulation enables efficient evaluation of the influence of force components on sensor response and constitutes a foundation for future load-identification approaches based on structural-response measurements.

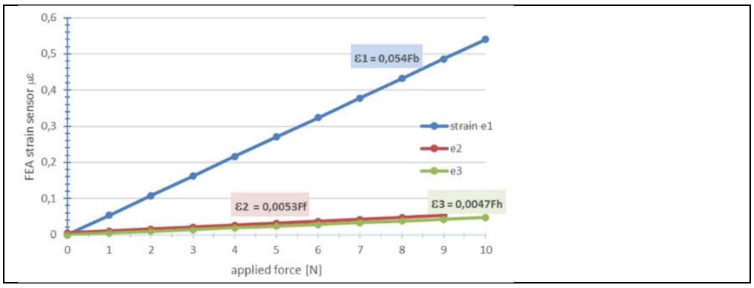

Fig. 9. Relationship between equivalent sensor strain and applied force components

5. MODEL VALIDATION AND DISCUSSION

To validate the proposed compliance-matrix-based model. the sensor response predicted by the FEM model was compared with the response recorded by the factory-installed M240 PCB sensor during actual abrasive waterjet cutting experiments.

The validation procedure consisted of two independent stages. In the first stage. cutting-force components F_b. F_f. and F_h were determined experimentally using the Kistler dynamometer. as described in Section 3. These force components were subsequently used as input loads for the FEM model of the cutting-head supporting structure.

In the second stage. the response of the M240 PCB sensor mounted on the cutting-head support was recorded during the cutting process. The experimentally measured sensor signal was then compared with the equivalent strain values predicted by the compliance-matrix-based FEM model. The measurement setup and the coordinate system adopted for the investigated cutting-head support are shown in Fig. 10.

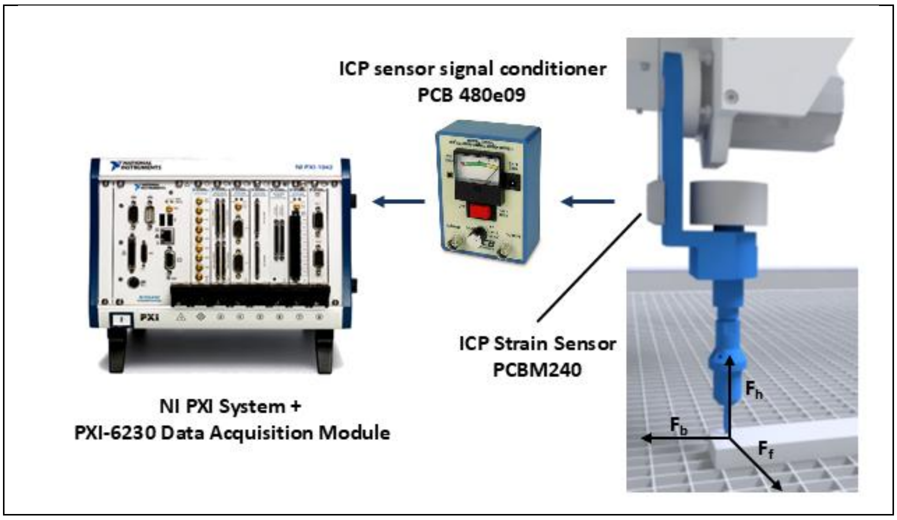

Fig. 10. Measuring station scheme and coordinate system of the cutter head

The relationship between the experimentally recorded sensor response and the force components determined from the cutting-force measurements is presented in Fig. 11. The coloured curves represent the experimentally measured equivalent strain responses ε_1. ε_2 and ε_3 associated with the force components F_b. F_f and F_h. respectively. The dashed trend lines indicate the corresponding linear approximations obtained from the experimental data and were introduced to facilitate comparison of the sensitivity of the sensor response in the individual loading directions.

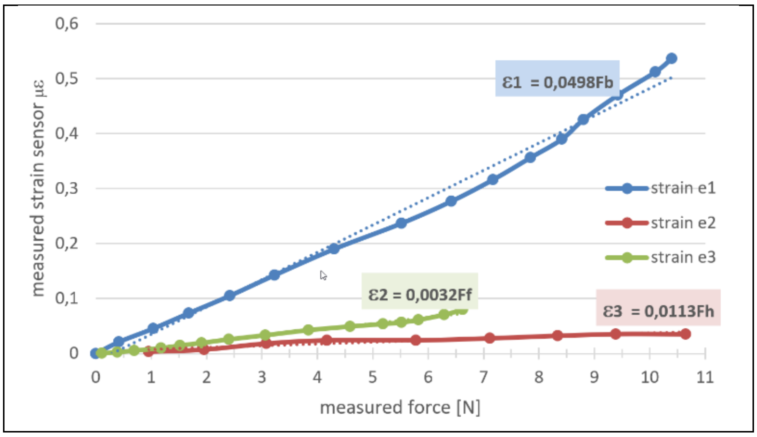

Fig. 11. Relationship between experimentally recorded sensor response and force components Fb. Ff and Fh determined from cutting-force measurements

A comparison between the numerical and experimental results shows a consistent trend. with a predominantly linear relationship between the applied forces and the sensor response (Figure 12). The highest quantitative agreement was obtained for the direction corresponding to the lowest structural stiffness (X direction. associated with F_b). where the relative error of the FEM-based prediction was approximately 8%. Figure 12 presents separate comparisons for the F_b and F_f force components. For the F_b direction. corresponding to the lowest stiffness of the supporting structure. the FEM prediction follows the experimental trend closely over the entire investigated load range. In contrast. for the F_f direction. larger deviations between the numerical and experimental results can be observed. Although the overall tendency remains similar. the reduced sensor sensitivity associated with the higher structural stiffness in this direction increases the uncertainty of the comparison.

In the remaining directions. characterized by higher structural stiffness. the sensitivity of the measurement system and the dispersion of experimental data limit the accuracy of the comparison. As a result. the influence of forces F_f and F_h cannot be unambiguously assessed within the considered load range.

The results indicate that the response of the cutting-head supporting structure is most sensitive to loading in directions corresponding to lower structural stiffness. For directions with significantly higher stiffness. improved measurement sensitivity or alternative sensor locations may be required to enhance the accuracy of structural-response identification.

The obtained results confirm that the proposed compliance-matrix-based approach is capable of describing the structural response of the investigated cutting-head support under process loading conditions. The study therefore demonstrates the feasibility of utilizing an existing machine-mounted sensor as a source of information about the deformation behaviour of the cutting-head support during abrasive waterjet cutting.

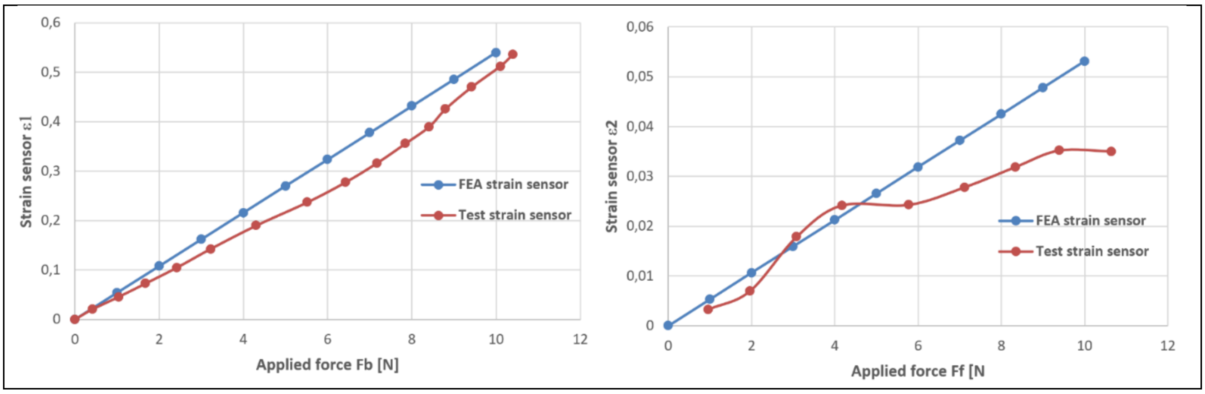

Fig. 12. Comparison between experimentally measured sensor response and FEM-based model predictions for F_b and F_f loading directions

6. CONCLUSION

Based on the conducted experimental investigations and numerical analyses. the following conclusions can be drawn:

• Experimental measurements of reaction forces during abrasive waterjet cutting demonstrated that the traverse speed significantly affects the force components. particularly the feed force and the force normal to the machined surface. The obtained data provide a reliable basis for defining loading conditions in numerical analyses.

• The proposed FEM model of the cutting head supporting structure enables a clear identification of the displacement response under loads applied in three orthogonal directions. The adopted idealization of the cutting head as a reference point allowed elimination of unnecessary nonlinearities and ensured a consistent interpretation of results.

• The application of a series of unit-load simulations enabled the determination of the compliance matrix. providing a compact mathematical description of the relationship between applied forces and the structural response of the cutting-head support. The developed model allows rapid prediction of sensor-related displacement responses for arbitrary force configurations within the linear range. without the need for repeated FEM analyses.

• The comparison of numerical and experimental results showed a consistent linear trend. The highest quantitative agreement was obtained for the direction corresponding to the lowest structural stiffness. where the relative error between the FEM-based prediction and the experimental measurement was approximately 8%.

• The piezoelectric strain sensor originally used for collision detection demonstrated potential as a source of information about the structural response of the cutting-head support during abrasive waterjet cutting. However. the effectiveness of this approach strongly depends on the directional stiffness of the structure and the sensitivity of the measurement system.

• The analysis revealed significant differences in structural stiffness along individual directions. In directions characterized by high stiffness. the sensor response was relatively small. which limits the sensitivity of structural-response measurements and increases the uncertainty of the comparison between numerical and experimental results.

• The results indicate that future research should focus on the design of a supporting structure with more uniform directional stiffness. Such a design would improve the sensitivity and directional consistency of the structural-response measurements. creating more favourable conditions for future force-identification methodologies. In this context. the application of structural optimization methods. particularly those combining FEM analysis with optimization algorithms. appears to be a promising approach.

The proposed methodology provides a basis for the development of advanced monitoring systems for AWJ cutting processes. The compliance-matrix-based framework offers a computationally efficient tool for describing the structural response of cutting-head support systems and may serve as a foundation for future indirect load-identification approaches and integration into intelligent machining systems.

REFERENCES

[1] NATARAJAN Y., MURUGESAN P.K., MOHAN M., KHAN S.A.L.A., 2020. *Abrasive Water Jet Machining Process – a State of Art Review*. Journal of Manufacturing Processes. 49, 271–322.

[2] KRAJCARZ D., BAŃKOWSKI D., MŁYNARCZYK P., 2017. *The Effect of Traverse Speed on Kerf Width in AWJ Cutting of Ceramic Tiles*. Science Direct. Procedia Engineering. 192, 469–473.

[3] AKKURT A., KULECKI M.K., SEKER U., ERCA F., 2004. *Effect of Feed Rate on Surface Roughness in Abrasive Waterjet Cutting Applications*. Journal of Materials Processing Technology. 147, 389–396.

[4] GUO Z., RAMULU M., JENKINS M.G., 2000. *Analysis of the Waterjet Contact Impact on Target Material*. Optics and Lasers in Engineering. 33, 121–139.

[5] LI H., LI J., HUANG Z., GUO CH., WANG H., LI W., 2025. *Numerical Investigation of Abrasive Water Jet Impact Force Characteristics by Using the Coupled SPH–FEM Method: Considering the Shape. the Interaction and the Fragmentation of Abrasive Particles*. Powder Technology. 465, 121287.

[6] AXINTE D.A., KONG M.C., 2009. *An Integrated Monitoring Method to Supervise Waterjet Machining*. CIRP Annals – Manufacturing Technology. 58, 303–306.

[7] HASSAN A.I., CHEN C., KOVACEVIC R., 2004. *On-Line Monitoring of Depth of Cut in AWJ Cutting*. International Journal of Machine Tools & Manufacture. 44, 595–605.

[8] LISSEK F., KAUFELD M., TEGAS J., HLOCH S., 2016. *Online Monitoring for Abrasive Waterjet Cutting of CFRP Via Acoustic Emission: Evaluation of Machining Parameters and Workpiece Quality Due to the Burst Analysis*. Procedia Engineering. 146, 67–76.

[9] RABANI A., MARINESCU I., AXINTE D., 2012. *Acoustic Emission Energy Transfer Rate – a Method for Monitoring Abrasive Waterjet Milling*. International Journal of Machine Tools & Manufacture. 61, 80–89.

[10] KARMIRIS-OBRATAŃSKI P., KARKALOS N.E., KUDELSKI R., PAPAZOGLOU E.L., MARKOPOULOS A.P., 2021. *Experimental Study on the Correlation of Cutting Head Vibrations and Kerf Characteristics During Abrasive Waterjet Cutting of Titanium Alloy*. Procedia CIRP. 101, 226–229.

[11] MONNO M., RAVASIO C., 2005. *The Effect of Cutting Head Vibrations on the Surfaces Generated by Waterjet Cutting*. International Journal of Machine & Manufacture. 45, 355–363.

[12] COPERTARO E., PEROTTI F., CASTELLINI P., CHIARIOTTI P., MARTARELLI M., ANNONI M., 2020. *Focusing Tube Operational Vibration as a Means for Monitoring the Abrasive Waterjet Cutting Capability*. Journal of Manufacturing Processes. 59, 1–10.

[13] PIETROW D., FAIRCLOUGH P.A., KERRIGAN K., 2024. *A Framework for Tool Condition Monitoring of Abrasive Waterjet Systems*. Procedia CIRP. 126, 475–480.

[14] COPERTARO E., 2022. *Assessment of Resistive Strain Gauges Measurement Performances in Experimental Modal Analysis and Their Application to the Diagnostics of Abrasive Waterjet Machinery*. Measurement. 188, 110626.

[15] YANG W., LI Z., LIU B., ZHANG B., MA P., 2026. *Comparative CFD–DEM Study of Granite Fracture Mechanisms Induced by Continuous. Pulsed and Abrasive Water Jets*. Powder Technology, 470, 122030.

[16] TORRUBIA P.L., AXINTE D.A., BILLINGHAM J., 2015. *Stochastic Modelling of Abrasive Waterjet Footprints Using Finite Element Analysis*. International Journal of Machine Tools & Manufacture. 95, 39–51.